Resolution of the forbidden ($J = 0 \rightarrow 0$) excitation puzzle in Mg-like ions.

L. Fernández-Menchero[1], G. Del Zanna[2], and N. R. Badnell[1]

[1] Department of Physics, University of Strathclyde. Glasgow G4 0NG, United Kingdom
e-mail: luis.fernandez-menchero@strath.ac.uk
[2] Department of Applied Mathematics and Theoretical Physics, University of Cambridge, Cambridge CB3 0WA, United Kingdom

Received ; accepted

ABSTRACT

We investigate the source of the discrepancy between *R*-Matrix and Distorted Wave collision strengths for $J - J' = 0 - 0$ transitions in Mg-like ions, e.g. $3s^2\,{}^1S_0 - 3p^2\,{}^1S_0$, as reported by Fernández-Menchero et al. (2014b). We find it to be due to the neglect of coupling, e.g. via $3s3p\,{}^1P_1$, as done by most distorted wave codes. We have implemented an option to account for such coupling within the AUTOSTRUCTURE distorted-wave code. This removes the factor ~ 10 and ~ 100 discrepancy for Fe^{14+} and S^{4+} respectively, for such transitions. The neglect of coupling would have affected (to some degree) the atomic data for a few weak transitions in other isoelectronic sequences, calculated with DW codes such as FAC and HULLAC. We compare the Fe^{14+} line intensities predicted with the *R*-matrix collision strengths against solar active region and flare observations, finding good agreement, hence confirming the reliability of the *R*-matrix calculations. For Fe^{14+}, we suggest that the best density diagnostic ratio is the 327.0/321.8 Å.

Key words. Atomic data – Techniques: spectroscopic

1. Introduction

In a recent paper (Fernández-Menchero et al. 2014b) we used the intermediate coupling frame transformation *R*-matrix method to calculate electron-impact excitation data for all ions of the Mg-like isoelectronic sequence, from Al^+ to Zn^{18+}, for all transitions involving levels up to principal quantum number $n = 5$. We also carried-out distorted wave (DW) calculations using the AUTOSTRUCTURE code (AS) (Badnell 2011) using exactly the same atomic structure as we used for the *R*-matrix calculations. We compared our AS-DW results, as well as those from other DW codes viz. the Flexible Atomic Code (FAC) (Gu 2003) by Landi (2011) and the UCL-DW code (Eissner 1998) by Christensen et al. (1985), with our *R*-matrix ones for Fe^{14+}. We found large differences between our *R*-matrix background collision strengths and those from AS-DW and FAC by Landi (2011) for some weak transitions, by an order of magnitude for the $J - J' = 0 - 0$ forbidden transition $3s^2\,{}^1S_0 - 3p^2\,{}^1S_0$. Conversely, the UCL-DW results of Christensen et al. (1985) were in broad agreement with the *R*-matrix ones. Clearly, the source of the difference must lie in the treatment of the (DW) scattering problem, not the description of the atomic structure.

It is important to understand the origin of such a large disagreement in the collision strengths calculated by different methods. Even today, the distorted wave method is still relied upon extensively for calculations of electron-impact data for excitation and ionization of atoms, ions and molecules. It is stored in databases such as CHIANTI[1] (Landi et al. 2013) and OPEN ADAS[2]. This data is then used in turn by plasma modellers to determine spectral diagnostics for both astrophysical and magnetic fusion plasmas.

[1] http://www.chiantidatabase.org
[2] http://open.adas.ac.uk

2. Methodologies

The *R*-Matrix close-coupling and DW methods solve the formal scattering equations for the colliding electron in their respective approximations (Eissner & Seaton 1972). Thence, they both calculate the elements of the reactance matrix K, which is related to the transmission matrix T via

$$T = \frac{-2\mathrm{i}K}{1 - \mathrm{i}K}\,, \tag{1}$$

and the resulting scattering matrix, $S = 1 - T$, is unitary. The collision strength (Ω_{ij}) and cross section (Q_{ij}) for any transition $i - j$ is then easily determined since

$$Q_{ij} \propto \Omega_{ij} \propto |T_{ij}|^2\,. \tag{2}$$

The *R*-matrix method solves the closely-coupled scattering equations and so naturally determines all elements of the K-matrix for a given set of target levels. A significant advantage of the DW method is that it does not need to calculate the entire K-matrix since it solves uncoupled scattering equations. Formally, it can make use of

$$T = \frac{-2\mathrm{i}K}{(1 - \mathrm{i}K)} \times \frac{(1 + \mathrm{i}K)}{(1 + \mathrm{i}K)} = \frac{-2\mathrm{i}K + 2K^2}{1 + K^2} \approx -2\mathrm{i}K\,, \tag{3}$$

for K small, which is usually the case for atoms which are several times ionized (Hayes & Seaton 1977).

In most astrophysical and magnetic fusion plasmas the main population of any given ion lies in its ground and metastable levels M. The main radiating properties of the full set of excited levels N are then determined by collisional excitation from levels M to N, followed by radiative cascade. The DW method then only needs to solve an $M \times N$ problem, for $M \ll N$, as opposed to the N^2 problem for the *R*-matrix method. Of course, the

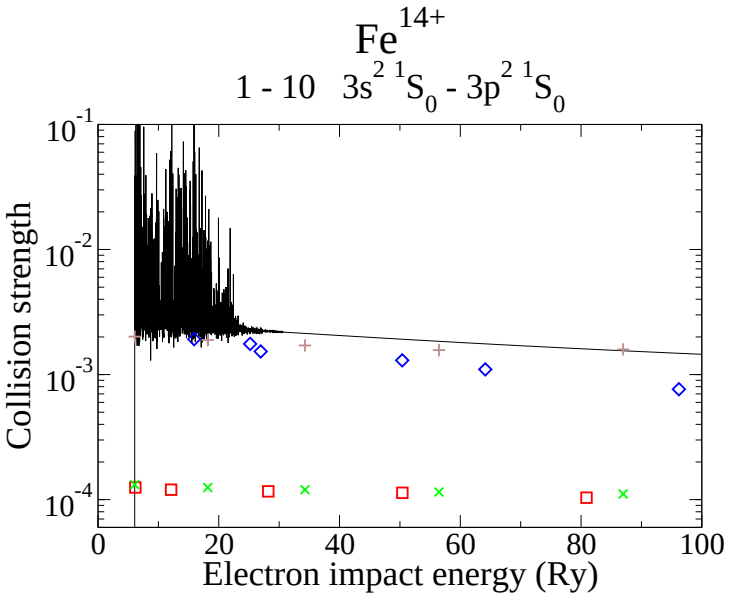

Fig. 1. Electron-impact excitation collision strength versus the impact energy for the transition $3s^2\ ^1S - 3p^2\ ^1S$ of Fe^{14+} . Full line: *R*-matrix (Fernández-Menchero et al. 2014b); ×: AS-DW (Fernández-Menchero et al. 2014b); +: AS-UDW (present work); □: FAC-DW (Landi 2011); ◇: UCL-DW (Christensen et al. 1985).

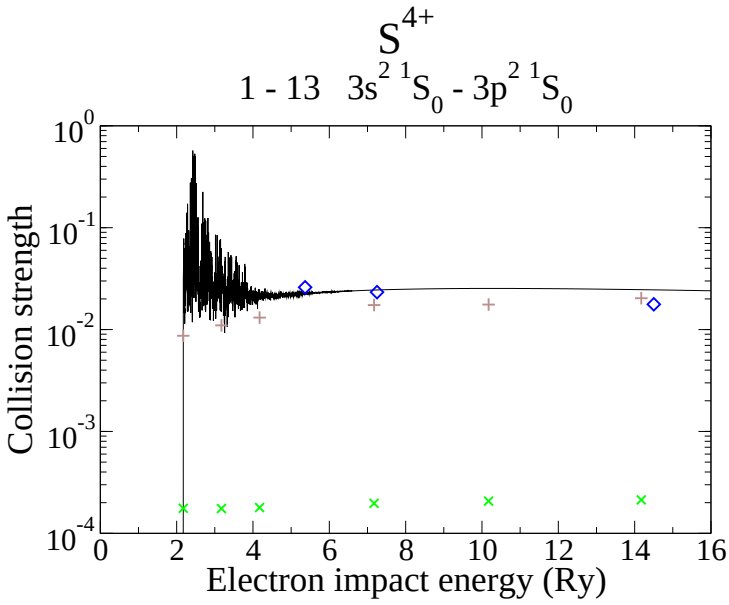

Fig. 2. Electron-impact excitation collision strength versus the impact energy for the transition $3s^2\ ^1S - 3p^2\ ^1S$ of S^{4+}. Full line: *R*-matrix (Fernández-Menchero et al. 2014b); ×: AS-DW (Fernández-Menchero et al. 2014b); +: AS-UDW (present work); ◇: UCL-DW (Christensen et al. 1986).

DW method normally neglects resonances but their contribution rapidly diminishes for more highly excited levels.

AS-DW, FAC and, indeed, HULLAC (Bar-Shalom et al. 1988) all make use of equation (3) and are said to be non-unitarized DW methods. However, the UCL-DW code has the option to use equation (1) and is said to be a unitarized DW method when it does so. We speculated (Fernández-Menchero et al. 2014b) that this might be the source of the differences in weak collision strengths for forbidden transitions since the use of equation (1) amounts to treating the close-coupling as a perturbation, while the use of (3) neglects it completely. Although AS-DW has the capability of calculating all elements of the *K*-matrix ($M = N$) it did so on-the-fly, the full matrix was never held. We have now implemented an option to retain the full *K*-matrix and so utilize equation (1) to give a unitarized method (AS-UDW).

3. Results

In Figs. 1, 2 we show the electron-impact excitation collision strength Ω for the transition $3s^2\ ^1S - 3p^2\ ^1S$ of the ions Fe^{14+} and S^{4+}. We compare the results of *R*-matrix and (non-unitarized) AS-DW calculations by Fernández-Menchero et al. (2014b) with the UCL-DW ones of Christensen et al. (1985) and FAC-DW of Landi (2011) for Fe^{14+} and UCL-DW of Christensen et al. (1986) for S^{4+}, and compare and contrast them with present (unitarized) AS-UDW results. The AS-(U)DW results were obtained using exactly the same target atomic structures as the *R*-matrix ones.

The results of Christensen et al. (1985) and Christensen et al. (1986) obtained with the UCL-DW code are quite close to the *R*-matrix ones, the differences can be attributed to the different atomic structures used. However, the FAC-DW results of Landi (2011) (Fe^{14+} only) and the AS-DW ones of Fernández-Menchero et al. (2014b) differ by large factors from the *R*-matrix ones for this transition: $\sim$ 10 for Fe^{14+} and $\sim$ 100 for the S^{4+}. However, the AS-UDW results show a dramatic increase over the non-unitarized ones, by very similar factors. This demonstrates that this transition is dominated ($\sim$ 90% and $\sim$ 99%) by coupling. It also shows that the original speculation of Fernández-Menchero et al. (2014b) that the results of Christensen et al. (1985) and Christensen et al. (1986) were obtained using the unitarized option of the UCL-DW code was correct.

We carried-out a series of calculations progressively reducing the number of target configurations included in the scattering calculation in order to determine the source of the coupling for the $3s^2\ ^1S - 3p^2\ ^1S$ transition. It was still present with a three configuration ($3s^2, 3s3p, 3p^2$) target expansion, but disappeared on omitting the 3s3p. Not too surprisingly, perhaps, the dominant coupling mechanism is thus the double dipole one: $3s^2\ ^1S \rightarrow 3s3p\ ^1P \rightarrow 3p^2\ ^1S$.

Given that the *R*-matrix and AS-(U)DW calculations used the same atomic structure, one might wonder about consistency of the high behaviour of the collision strengths: *R*-matrix and AS-UDW should tend to the same Born limit as the non-unitarized AS-DW. As demonstrated by Fernández-Menchero et al. (2014b), a reduced Burgess–Tully diagram (Burgess & Tully 1992) shows that the *R*-matrix collision strength 'turns-over' at high energy and heads down to the same limit as the AS-DW one. The present AS-UDW results follow the same behaviour at high energy as the *R*-matrix ones.

3.1. Comparison to observations for Fe^{14+}

We have seen the large differences in the collision strengths of the 1–10 $3s^2\ ^1S - 3p^2\ ^1S$ transition in Fe^{14+}. It is therefore useful to validate our *R*-matrix results against observations. As briefly discussed in Fernández-Menchero et al. (2014b), a significant fraction of the population of the upper level 10 $3p^2\ ^1S$ is due to the above transition, the direct excitation from the ground state. This upper level mainly decays with an allowed transition to level 5, $3s3p\ ^1P^o_1$.

Therefore, the intensity of the 5–10 transition is directly affected by the collision strength of the above 1–10 $3s^2\ ^1S - 3p^2\ ^1S$ transition, so we calculated the level populations for this ion using our atomic data (Fernández-Menchero et al. 2014b), to com-

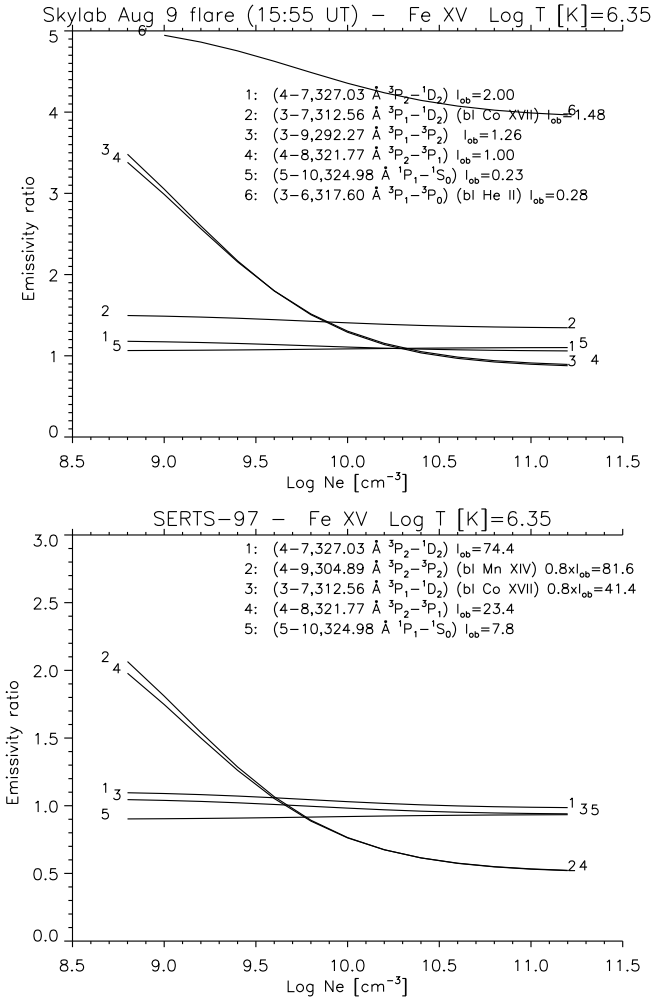

Fig. 3. Emissivity ratio plots for some Fe^{14+} EUV lines observed by Skylab (above) and SERTS-97 (below).

pare the relative intensity of the 5–10 transition to those of other lines.

The 5-10 transition turned out in itself to be a troublesome line, in terms of its identifications. This transition (together with other lines) was identified by Churilov et al. (1985) using laboratory spectra with a line observed at 324.98 Å. The identifications were mainly based on wavelength coincidences (the line intensities were not calibrated). There were previous suggestions that a solar line at 323.57 Å was instead due to this transition (Cowan & Widing 1973), so Keenan et al. (1993) considered Skylab S082A intensities of several solar flares, to assess if the identification was correct. The Skylab observations confirmed the Churilov et al. (1985) identification, although there is a large scatter in the intensity of this line, which is always weak in the solar spectra. The 324.98 Å line was invisible in the active region SERTS-89 spectra of Thomas & Neupert (1994), which led Young et al. (1998) to suggest that the identification of the 324.98 Å line as the 5–10 transition was probably not correct.

One way to compare at once the observed intensities of several lines with the predicted ones is to plot the 'emissivity ratios' (Del Zanna et al. 2004), which are basically the ratios of the observed ($I_{\rm ob}$, energy units) and the calculated line emissivities as a function of the electron density $N_{\rm e}$:

$$R_{ji} \;=\; \frac{I_{\rm ob} N_{\rm e} \lambda_{ji}}{N_j(N_{\rm e}, T_{\rm e})\, A_{ji}}\, C\,, \qquad (4)$$

where $N_j(N_{\rm e}, T_{\rm e})$ is the population of the upper level j relative to the total number density of the ion, calculated at a fixed temperature $T_{\rm e}$ (the ratios of the lines considered here have little temperature sensitivity, and we have taken as $T_{\rm e}$ the value of peak ion abundnace in ionisation equilibrium); λ_{ji} is the wavelength of the transition, A_{ji} is the spontaneous radiative transition probability, and C is a scaling constant that is the same for all the lines within one observation. If agreement between experimental and theoretical intensities is present, all lines should be closely spaced or intersect, for a near isodensity plasma. The value of C is chosen so that the emissivity ratios R_{ji} are near unity where they intersect.

If we consider the first of the flares considered by Keenan et al. (1993) and plot the emissivity ratios as a function of density, we obtain the results shown in Fig. 3 (top). There is excellent (to within a relative few percent) agreement bewteen observed and predicted intensities for the 327.0, 292.3, 321.8, 325.0 Å lines, at a density of $10^{10.3}$ cm^{-3}, in excellent agreement with the densities obtained from other ions. This is an improvement over the atomic data used at the time by Keenan et al. (1993). The 312.6 Å line is known to be blended (probably with Co XVII), and the 317.6 Å has been known to be severely blended (possibly with Na VI).

There are various other EUV observations of the Fe XV lines, but often spectra have not been properly calibrated, did not have enough resolution or sensitivity (the 325.0 Å line is weak). There is however a well calibrated SERTS-97 spectrum (Brosius et al. 2000) where the 325.0 Å line was visible. Most of the lines listed as due to Fe XV turn out to be severely blended, however good agreement is found in the intensities of the 327.0, 321.8, and 325.0 Å lines, as shown in Fig. 3 (bottom). As already mentioned, the 312.6 Å is known to be blended with Co XVII, while the 304.9 Å line is possibly blended with Mn XIV. Similar results were obtained (using different atomic data) by Keenan et al. (2005). We also considered the SERTS-94 spectrum, where more lines were observed (but not the 5-10 transition), finding overall good agreement between theory and observation.

In conclusion, the few solar observations of the 5-10 line show very good agreement between the observed and predicted intensity of this line, which confirms the reliability of the *R*-matrix calculations.

Finally, we note that Keenan et al. (1993) suggested that the 325.0 Å transition would be an excellent density diagnostic for the solar corona; however, the 327.0 Å line has a similar sensitivity at typical active region/flare densities, so it is to be preferred because it is much stronger. We suggest that the best diagnostic ratio for Fe XV is the 327.0/321.8 Å. The lines are both strong, unblended and nearby in wavelength.

3.2. Other sequences

What about systems other than Mg-like? The obvious one is Be-like — the $n = 2$ analogue: $2s^2, 2s2p, 2p^2$. In Fig. 4 we show the *R*-matrix collision strengths of Fernández-Menchero et al. (2014a) for O^{4+} (the same residual charge as Mg-like S) and compare them with the present non-unitarized and unitarized AS-(U)DW results, calculated with the same atomic structure. We see that that *R*-matrix background collision strengths and the

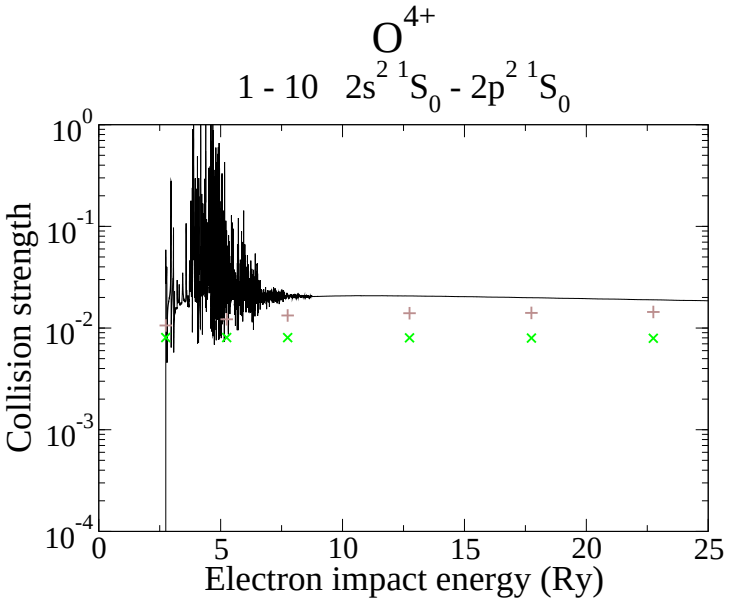

Fig. 4. Electron-impact excitation collision strength versus the impact energy for the transition $2s^2\,{}^1S - 2p^2\,{}^1S$ of O^{4+}. Full line: *R*-matrix (Fernández-Menchero et al. 2014a); ×: AS-DW (present work); +: AS-UDW (present work).

AS-UDW are similar in in magnitude to the S^{4+} ones shown in Fig. 2. In contrast, however, the non-unitarized AS-DW results are much larger than in the corresponding S case — neglect of coupling only reduces them by a factor of ~ 2 instead of ~ 100. The reason for this, it turns out, is that the $2s^2$ is more strongly mixed with the $2p^2\,{}^1S$ than in the corresponding $n = 3$ case. There is enough admixture of $2s^2$ in the $2p^2\,{}^1S$ state for it to proceed directly through the target mixing. In contrast, the $3p^2\,{}^1S$ state is pure enough that very little collision strength arises directly.

Since the transition $J - J' = 0 - 0$ takes place through target state mixing, which is small in general, the total collision strength is expected to be strongly sensitive to small changes in the atomic structure. We have found that making small changes in the atomic structure, so that the mixing coefficients change, can change the collision strength calculated with AS-DW by a factor 10, while the one calculated with AS-UDW remains much more stable (to within $\sim 20\%$).

We have detected this coupling effect only in very weak optically forbidden transitions ($J - J' = 0 - 0$). In the coronal approximation, where the population of an ion is concentrated in the ground state, in general, the population of such upper states does not come from a direct excitation from the ground state, but from radiative cascading from more excited ones. However, the $3p^2$ case, being a double electron jump from the ground, is only populated weakly by cascade. In higher density plasmas ($\gtrsim 10^{14}$ cm^{-3}), such as magnetic fusion, the $3s3p\,{}^3P_2$ population can be expected to drive the $3p^2\,{}^1S$ population by direct excitation.

4. Conclusion

We have implemented an option in the AS-DW code to convert the reactance *K*-matrices to the transmission *T*-matrices which gives rise to unitary scattering *S*-matrices — AS-UDW. Physically, this corresponds to treating all coupling of the scattering equations as a perturbation. The effect of coupling is very large for select transitions: $J = 0 - 0$ in Mg-like ions.

The neglect of coupling is the reason for the large differences found in Fernández-Menchero et al. (2014b) for such transitions between *R*-matrix and distorted wave results, including those which used the exact same atomic structure. The implementation of AS-UDW corrects for this difference.

We compared the theoretical line intensities obtained using the *R*-matrix results for Mg-like iron with solar observations and found good agreement, confirming the reliability of the calculations.

Finally, we point out that the neglect of coupling would have affected (to some degree) the atomic data for a few weak transitions in other isoelectronic sequences, calculated with DW codes such as FAC and HULLAC.

Acknowledgements. The present work was funded by STFC (UK) through the University of Strathclyde UK APAP network grant ST/J000892/1 and the University of Cambridge DAMTP astrophysics grant.

References

Badnell, N. R. 2011, Comput. Phys. Commun., 182, 1528
Bar-Shalom, A., Klapisch, M., & Oreg, J. 1988, Phys. Rev. A, 38, 1773
Brosius, J. W., Thomas, R. J., Davila, J. M., & Landi, E. 2000, Astrophys. J., 543, 1016
Burgess, A. & Tully, J. A. 1992, Astron. Astrophys., 254, 436
Christensen, R. B., Norcross, D. W., & Pradhan, A. K. 1985, Phys. Rev. A, 32, 93
Christensen, R. B., Norcross, D. W., & Pradhan, A. K. 1986, Phys. Rev. A, 34, 4704
Churilov, S. S., Kononov, E. Y., Ryabtsev, A. N., & Zayikin, Y. F. 1985, Phys. Scr., 32, 501
Cowan, R. D. & Widing, K. G. 1973, Astrophys. J., 180, 285
Del Zanna, G., Berrington, K. A., & Mason, H. E. 2004, Astron. Astrophys., 422, 731
Eissner, W. 1998, Computer Physics Communications, 114, 295
Eissner, W. & Seaton, M. J. 1972, Journal of Physics B: Atomic and Molecular Physics, 5, 2187
Fernández-Menchero, L., Zanna, G. D., & Badnell, N. R. 2014a, Astron. Astrophys., 566, A104
Fernández-Menchero, L., Zanna, G. D., & Badnell, N. R. 2014b, Astron. Astrophys., 572, A115
Gu, M. F. 2003, Astrophys. J., 590, 1131
Hayes, M. A. & Seaton, M. J. 1977, Journal of Physics B: Atomic and Molecular Physics, 10, L573
Keenan, F. P., Aggarwal, K. M., Milligan, R. O., et al. 2005, Mon. Not. R. Astr. Soc., 356, 1592
Keenan, F. P., Dufton, P. L., Conlon, E. S., et al. 1993, Astrophys. J., 405, 798
Landi, E. 2011, At. Data Nucl. Data Tables, 97, 587
Landi, E., Young, P. R., Dere, K. P., Zanna, G. D., & Mason, H. E. 2013, Astrophys. J., 763, 86
Thomas, R. J. & Neupert, W. M. 1994, ApJS, 91, 461
Young, P. R., Landi, E., & Thomas, R. J. 1998, A&A, 329, 291